RC22292 (W0201-025) January 3, 2002
Materials Science

IBM Research Report

Thermal Transformation of ZrO2, HfO2, and Al2O3 Mixed Oxide Films Deposited by Chemical Solution Deposition

Deborah Neumayer, Eduard Cartier
IBM Research Division
Thomas J. Watson Research Center
P.O. Box 218
Yorktown Heights, NY 10598

Research Division
Almaden - Austin - Beijing - Delhi - Haifa - India - T. J. Watson - Tokyo - Zurich

THERMAL TRANSFORMATION OF ZRO_2, HFO_2 AND AL_2O_3 MIXED OXIDE FILMS DEPOSITED BY CHEMICAL SOLUTION DEPOSITION

DEBORAH A. NEUMAYER, E. CARTIER,
IBM, T.J. Watson Research Center, P.O. Box 218, Yorktown Heights, NY 10598

ABSTRACT

The thermal stability, and microstructure of zirconium aluminum oxide (ZAO) and hafnium aluminum oxide (HAO) mixed oxides were evaluated. The films were prepared by chemical solution deposition (CSD) using a solution prepared from zirconium, or hafnium butoxyethoxide, and aluminum butoxyethoxide dissolved in butoxyethanol. The films were spun onto SiO_xN_y coated Si wafers and furnace annealed at temperatures from 500-1200 ^oC in oxygen for 30 minutes. The microstructure and electrical properties of ZAO and HAO films were examined as a function of Zr/Al and Hf/Al ratio and annealing temperature. The films were characterized by X-ray diffraction, FTIR, RBS and AES. Crystallization/phase separation of ZrO_2 and HfO_2 in ZAO and HAO films was observed to be concentration and annealing temperature dependent. At low ($\leq$25%) ZrO_2 or HfO_2 concentrations at anneal temperatures less than 900 ^oC, an amorphous γ-alumina like material was observed in the ZAO and HAO films. Phase partitioning of the ZAO and HAO films was observed at higher ZrO_2 or HfO_2 concentrations and at higher anneal temperatures. Addition of Al_2O_3 to ZrO_2 or HfO_2 was found to increase the crystallization temperature of tetraganol ZrO_2, enable the formation of the tetragonal HfO_2 phase and increase the annealing temperature at which transformation of the tetragonal to monoclinic phase of ZrO_2 or HfO_2 is observed. Transformation from the tetragonal to the monoclinic phase was observed to occur more readily at lower temperatures in HAO films than ZAO films. Evidence of enhanced oxygen conduction at elevated temperatures was observed for 90% Hf 10% Al mixed oxide films.

INTRODUCTION

In the quest for improved performance, CMOS circuits are becoming denser and the CMOS devices smaller. The most common gate dielectric has been SiO_2. Recently SiO_2/Si_3N_4 combinations have begun to gain interest as a replacement for pure oxide. However, as the thickness of SiO_2 and SiO_2/Si_3N_4 stack films approach 10-20 Å substantial problems appear, including large leakage currents through the gate dielectric, concerns about the long term dielectric reliability, and difficulty of manufacture and thickness control. A solution to the problem is to use thick dielectric films having high dielectric constants (high K). Thus, investigation of alternate gate oxides such as Al_2O_3, ZrO_2, HfO_2, and mixed oxides such as zirconium and hafnium silicon oxide have been undertaken.[1] Al_2O_3, ZrO_2, and HfO_2 are reported to be thermodynamically stable in contact with silicon.[2] ZrO_2 doped Al_2O_3 and zirconium aluminum oxide (ZAO) has been considered as a gate oxide replacement.[3,4] In this study, we have utilized butoxyethoxide based chemical solution deposition (CSD) route as a quick and inexpensive means of screening ZAO and HAO. Unlike chemical vapor deposition or physical vapor deposition, CSD requires no vacuum equipment, no deposition tool development, and no process development time to obtain desired stoichiometry (solution concentration is film concentration). By utilizing a stable butoxyethoxide based chemistry with no aging effects, solutions can be prepared and stored indefinitely between spinnings and still obtain the same quality film.[5,6] Bulk powders of ZAO have been prepared by CSD with different solution chemistries,[7,8,9,10,11,12,13] However, no report exists describing the deposition of films of HAO or ZAO utilizing a butoxyethoxide CSD chemistry. In an attempt to gain a better understanding of the materials properties of ZAO and HAO we have prepared films of varying compositions of ZAO and HAO and characterized their thermal stability and microstructural properties.

EXPERIMENTAL

Chemical Solution Deposition of ZAO and HAO

Zirconium aluminum oxide and hafnium aluminum oxide (HAO) mixed oxides of various compositions in the $xZr(100-x)AlO_y$ (Z_xAO, x = 17, 50 %), where x =17 is labeled as $Z_{17}AO$, x= 50 is labeled as $Z_{50}AO$, and similarily for the $xHf(100-x)AlO_y$ (H_xAO, x= 25, 54, and 90) films were fabricated by CSD. The CSD solutions were prepared from a mixture of zirconium, hafnium and aluminum butoxyethoxides dissolved in butoxyethanol.[5-6] The films were deposited by spin casting on (5-20 Å) SiO_xN_y coated Si substrates. The Zr/Al and Hf/Al ratio was varied by mixing either a Zr or Hf butoxyethoxide solution and a separate Al butoxyethoxide. Solution composition was determined by ICP analysis by Galbraith Laboratories. After preparing spinning solution and loading the spinning solution into a syringe, 0.45 and 0.1 μm syringe filters were attached to the syringe and the spinning solution was syringed on the substrate until completely wetted. The substrate was then spun for 20 sec at 2000-4000 rpm onto a SiO_xN_y coated Si substrate which had been preheated on a 350 ^oC hot plate. After each spin-coating, the samples were baked on a hot plate at 150 ^oC for 1-3 min, then at 350 ^oC for 3-10 minutes in air. ZAO and HAO film thickness was varied by solution concentration, by spinning speed, and by depositing multiple layers with a hot plate bake anneal between each layer. The final film was hot plate baked at 350 ^oC for a minimum of 30 minutes before furnace annealing at 400, 500, 700, 800, 900, 1000, or 1100 ^oC for 30 min or 1200 ^oC for 60 min in flowing oxygen.

ZAO and HAO Film Characterization

X-ray diffraction (XRD) spectra were obtained using a Philips PW1729 diffractometer with Cu Kα radiation. The FTIR spectra were recorded with a Nicolet Nexus 670 spectrometer using DTGS KBR detector and KBR beam splitter for mid-IR (4000-400 cm^{-1}) and using a DTGS

polyethylene detector and a solid substrate beam splitter for far-IR (600-50 cm^{-1}) data collection. The background for each spectrum was a piece of uncoated wafer that the ensuing films were spun on. To minimize fringing effects and internal reflections, background and spectra were collected at ~30° angle from the incident beam. The spectrum were analyzed using OMNIC v. 5.2 (Nicolet). After annealing at temperatures ≥ 800 °C, absorption bands attributable to SiO_2 at 1180 cm^{-1} and 1080 cm^{-1} from the LO and TO components of the asymmetric stretch of the SiO_4, 810 cm^{-1} band attributed to skeletal network Si-O-Si symmetric stretching, and a band at 460 cm^{-1} attributed to skeletal network Si-O-Si symmetric bending was observed in the FTIR spectra. Therefore, a representative thermal SiO_2 spectra was subtracted from the ZAO and HAO spectrums of all films discussed in this paper annealed at 800, 900, 1000, 1100 and 1200 °C using the subtraction feature of the OMNIC v. 5.2 software. For FTIR and X-ray diffraction (XRD) analysis, film thickness were at least 1000 Å thick. Film thickness was determined by n&k analysis (n&k analyzer, n&k Technology, Santa Clara, Ca)[14] and confirmed by single wavelength ellipsometry. Electric properties were measured using backside contact with In/Ga or thermally evaporated Al and topside contact with thermally evaporated Al dots. The two types of electrodes yield similar electrical response apart from the flat band shift due to the work function difference of the metals. An average dielectric constant from a minimum of three different films at thickness varying from 500-4000 Å is reported. No dependence of thickness on dielectric constant was observed.

RESULTS and DISCUSSION

X-ray diffraction (XRD) was performed at room temperature on undoped Al_2O_3, ZrO_2 and HfO_2 films after annealing hot plate baked (350 °C 30 minutes in air) films at 400, 500, 700, 800, 900, 1000, 1100 °C for 30 minutes and 1200 °C for 60 minutes in flowing oxygen. The results are summarized in Table 1. No evidence of any crystalline alumina phases was observed in the XRD

for undoped alumina films annealed at temperatures < 1200 °C, after annealing at 1200 °C for 60 minutes peaks attributable to α-alumina was observed. XRD spectra of annealed pure ZrO_2 and HfO_2 agreed with earlier published results,15 crystallization of alumina free tetragonal ZrO_2 was observed after annealing at 500 °C, partial transformation from tetragonal to monoclinic ZrO_2 was observed in the XRD spectra after annealing at 800-900 °C, only monoclinic ZrO_2 was observed in the XRD spectra after annealing at 1000-1200 °C. Crystallization of HfO_2 differed, in that, only monoclinic HfO_2 was observed after annealing at 500 -1200 °C.

X-ray diffraction was performed at room temperature on zirconium aluminum oxide and hafnium aluminum oxide on various compositions in the $xZr(100-x)AlO_y$ where x =17 is labeled as $Z_{17}AO$, x= 50 is labeled as $Z_{50}AO$, and similarily for the $xHf(100-x)AlO_y$ (H_xAO, x= 25, 54, films. X-ray diffraction was performed at room temperature on $Z_{17}AO$, and $Z_{50}AO$ (zirconium aluminum oxide) and $H_{25}AO$, $H_{54}AO$, and $H_{90}AO$ (hafnium aluminum oxide) binary oxides after annealing hot plate baked (350 °C 30 minutes in air) films at 500, 700, 800, 900, 1100 °C for 30 minutes and 1200 °C for 60 minutes in flowing oxygen. A typical series of XRD diffraction patterns are shown in Figure 1 for $H_{25}AO$. At 800 and 900 °C, no XRD peaks are observed, characteristic of an amorphous film, after annealing at 1000 and 1100 °C, peaks attributable to tetragonal HfO_2 are observed and after annealing at 1200 °C, peaks attributable to monoclinic HfO_2 are observed. Similar results were observed in the $Z_{17}AO$, and $Z_{50}AO$ and $H_{25}AO$, $H_{54}AO$, and $H_{90}AO$ films. The annealing temperatures at which tetragonal and monoclinic ZrO_2 and HfO_2, and θ and α alumina are observed by XRD or FTIR spectra are listed in Table I.

As observed by XRD and in agreement with earlier results,[7-13,16,17,18,19] we have observed that combination of ZrO_2 with alumina in the ZAO films delayed crystallization of tetragonal ZrO_2 from 500 °C to at least 800 °C, and that transformation of the tetragonal to the monoclinic phase was delayed from 900 °C to at least 1200 °C. As listed in Table I, $Z_{50}AO$ converted from

tetragonal to monoclinic after annealing at 1200 °C for 60 minutes and $Z_{17}AO$ did not convert. No reports of HAO deposited by CSD are found in the literature. However, we have observed in agreement with the ZAO results, that combination of HfO_2 with Al_2O_3 in the $H_{25}AO$, $H_{54}AO$, and $H_{90}AO$ films enabled the formation of the tetragonal phase of HfO_2 which crystallized at a lower annealing temperatures than the monoclinic HfO_2 phase. The presence of the tetragonal HfO_2 or ZrO_2 in the HAO or ZAO films at lower temperatures than the monoclinic phase might be explained by the presence of Al_2O_3 hindering the grain growth of HfO_2 or ZrO_2 preventing the attainment of the critical particle size necessary for the tetragonal-monoclinic transformation.[4, 7, 11,13, 15-18]

FTIR

The FTIR spectrum of undoped Al_2O_3 annealed at 400, 500, 700, 800, 900, 1100 °C for 30 minutes and 1200 °C for 60 minutes in flowing oxygen were collected and peaks assigned according to the literature.[19-35] In the FTIR spectrum of Al_2O_3 after annealing at 400-1100 °C (Figure 2), a broad absorption band between 3700 and 3000 cm^{-1} is observed and assigned to O-H stretching vibrations. The broadness of the OH band is indicative of great local disorder.[20] The center of this O-H band shifts upwards from 3372 cm^{-1} to 3546 cm^{-1} and the intensity decreases as the annealing temperature was increased from 400 to 1100 °C. The upward shift of the center of the OH absorption band agrees well with a loss of hydrogen bonding between adjacent layers with observed vibrational modes 3500-3300 cm^{-1} and the retention of stronger hydrogen bonds between hydroxy groups lying in the same plane with vibrational modes observed at higher frequencies, 3600-3500 cm^{-1}.[21] However, the OH band does not completely disappear until alumina has converted to the α phase after annealing at 1200 °C for 60 minutes. Weak absorption bands at 2957, 2925, and 2850 cm^{-1} associated with C-H stretch are observed and attributed to residual organics in the film. These bands persisted even after annealing at 1200 °C for 60

minutes and suggest the inclusion of organic fragments in the alumina network. Further support for trapped organic fragments is provided by the observation of a weak absorption band at 2337 cm^{-1} which is assigned to trapped CO_2 in the film.[22,23] The intensity of the trapped CO_2 band increases with annealing temperature from 700-1100 ^oC and then decreases after annealing at 1200 ^oC. This band probably arises from pyrolysis of trapped organics in the film. The absorption bands in the spectral region between 1700-1200 cm^{-1} attributed to adsorbed water, organics and carbonates in the film were observed to decrease in intensity and vary peak position as the annealing temperature is increased. A band at 1630 cm^{-1} is assigned to the H-OH bending vibration of adsorbed water in the film.[19,20,23,24,28,32,33] In the films annealed at 400 ^oC, absorption bands at 1557, 1464, 1413, and 1345 cm^{-1} were observed; in the films annealed at 500-800 ^oC annealed films, only a broad absorption between 1700-1300 cm^{-1} is observed, indicative of a disordered microstructure and in the films annealed at 1000 and 1100 ^oC, absorption bands at 1596, 1527, 1446, and 1345 cm^{-1} are observed. These bands are attributed to water, organics and/or carbonates in the film.[19,20,24,2528,32,33] In the film annealed at 1200 ^oC, none of these absorption bands are observed. In the films annealed at 350-800 ^oC, a broad two centered absorption band is observed between 1000-200 cm^{-1}. This two centered band with approximately equal intensity bands has one center at ~650-700 cm^{-1} and one at 590 cm^{-1} with a shoulder at 410 cm^{-1}. This two centered broad band is characteristic of γ-alumina.[26,27,28,29,30] The broadness absorption band is indicative of the disorder in the microstructure and is attributed to a wide range of Al-O stretching modes for octahedral, AlO_6 and tetrahedral, AlO_4 units and complex interactive vibrations.[26-30] Generally, absorbance in the region 700-950 cm^{-1} is associated with tetrahedral sites in alumina and absorbance less than 700 cm^{-1} is associated with octahedral sites in alumina.[19,20,25,31] After annealing at 1000 ^oC and 1100 ^oC, the two centered broad band no longer has approximately equal intensity bands, the strong absorption band centered at 540 cm^{-1}

increases in intensity, distinctive vibrational modes appear which are consistent with formation of θ-Al_2O_3.[26-29] The growth in intensity of the band centered at 540 cm^{-1} is most likely associated with the conversion of tetrahedral to octahedral sites in the alumina which accompanies the γ–θ phase transition. After annealing at 1200 °C, absorption bands attributable to α-Al_2O_3 are observed at 635 (medium), 567 (strong), 501 (medium), 435 (strong) and 383 cm^{-1} (medium) and the lack of absorptions below 700 cm^{-1} is consistent with the complete conversion of tetrahedral to octahedral sites in α-Al_2O_3. [26-29, ,32]

The FTIR spectra of Z_{17}AO and Z_{50}AO, H_{25}AO, H_{54}AO, and H_{90}AO binary oxides baked at 350 °C in air on a hot plate for 30 minutes are shown in Fig. 3. The peaks in the ZAO and HAO spectra have been assigned according to the literature.[14,19-35] The broad band between 3700 and 3000 cm^{-1} is assigned to O-H stretching vibrations. The band at 1630 cm^{-1} and 1580 cm^{-1} is assigned to the H-OH bending vibration of adsorbed water in the film[19,20,23,24,28,32,33] The bands at 1450 and 1420 cm^{-1} are attributed to residual carbonates in the film. A band at 1100 cm^{-1} is attributed to the symmetrical Al-OH bending modes.[19,20,23,28, 33,34] Increasing ZrO_2 or HfO_2 content decreases the intensity of the bands at 3400, and 1630 associated with absorbed water in the film. From surface area studies of ZrO_2-Al_2O_3 powders, it is known that addition of ZrO_2 decreases total surface area of ZrO_2-Al_2O_3 powders indicative of a denser microstructure.[7,9,13] This reduction in surface area may account for the reduction in OH and HOH in the films with increasing ZrO_2 and HfO_2 content. In the Z_{17}AO and H_{25}AO films, a broad two centered absorption band is observed between 1000-200 cm^{-1}. This two centered band with approximately equal intensity bands has one center at ~650-700 cm^{-1} and one at 590 cm^{-1} with a shoulder at 410 cm^{-1} and is characteristic of γ-alumina.[26-30] In the Z_{50}AO, H_{54}AO, and H_{90}AO films, a broad absorption band is observed between 1000-200 cm^{-1} centered at 440 cm^{-1} with a shoulder at 670 cm^{-1} and is attributed to a mixture of amorphous ZrO_2 or HfO_2 and γ-alumina.

To gain a better understanding of the microstructural transformations occurring in the ZAO and HAO films during annealing at elevated temperatures, FTIR spectra were collected from $Z_{17}AO$ (Fig. 4), and $Z_{50}AO$ (Fig. 5) and $H_{25}AO$ (Fig. 6), $H_{54}AO$(Fig. 7) and $H_{90}AO$(Fig. 8) films annealed for 30 minutes in oxygen at 500, 700, 800, 900, 1000, 1100 ^oC for 30 minutes and 1200 ^oC for 60 minutes in flowing oxygen. A progressive change in the FTIR spectrum is observed as the annealing temperature is increased. As the annealing temperature is increased, the absorption bands associated with residual organics in the films decrease in intensity. A band at 2337 cm^{-1} is observed in the FTIR spectrum after annealing at 700-1200 ^oC and is assigned to trapped CO_2 in the film.[22,23] The intensity of the trapped CO_2 band increases with annealing temperature from 700-1000 ^oC and then decreases after annealing at 1100 and 1200 ^oC. This band probably arises from pyrolysis of organics in the film. However, the complete loss of residual organics from 17%, and $Z_{50}AO$ and $H_{25}AO$, 54% and $H_{90}AO$ films is not observed even after annealing at 1200 ^oC for 60m. As the annealing temperature is increased, the absorption bands associated hydroxyl and adsorbed water in the films decrease in intensity and the center of the OH absorption band to shifts 37-90 cm^{-1} upward from ~ 3400 to ~3490 cm^{-1}. A weak peak at 1106 cm^{-1}, with a shoulder at 1260 cm^{-1} is observed after annealing at 350-700 ^oC and not after annealing at 800-1200 ^oC and is assigned to the symmetrical and antisymmetrical Al-OH bending modes, respectively. [19,20,23,24,28,32,33] However, the complete loss of OH and H_2O from $Z_{17}AO$ and $Z_{50}AO$, $H_{25}AO$, $H_{54}AO$, and $H_{90}AO$ films is only observed after annealing at 1200 ^oC for 60m.

Dependence of the microstructure on stoichiometry and process conditions is most clearly seen in the FTIR spectrum from 1000-200 cm^{-1} which corresponds with M-O vibrations. In the $Z_{17}AO$ films (Fig. 4) and $H_{25}AO$ films (Fig. 6) annealed at 350-900 ^oC, a broad two centered absorption band between 1000-200 cm^{-1} with one center at ~630-680 cm^{-1} and one center at ~540-570 cm^{-1} and a shoulder at ~420 cm^{-1} characteristic of γ-alumina[26-30] is observed and is

nearly identical to the observed FTIR spectrum of undoped Al_2O_3 annealed at 350-800 ^oC (Figure 2). The nearly identical FTIR spectrum of the pure Al_2O_3 film compared to the $Z_{17}AO$ and $H_{25}AO$ films is indicative of interspersion of Zr and Hf throughout the amorphous alumina network. However as the anneal temperature is increased, phase partitioning is observed in the $Z_{17}AO$ films and $H_{25}AO$ films. After annealing $Z_{17}AO$ at 1000 ^oC, a strong absorption band centered at ~490 cm^{-1} with a shoulder at 394 cm^{-1} and a very weak absorption band ~180 cm^{-1} is observed and is consistent with formation of tetragonal ZrO_2. As the annealing temperature is increased to 1100 and 1200 ^oC, distinctive vibrational modes attributable to θ-alumina are observed on the broad absorption band. The resultant FTIR spectrum are attributed to a mixture of tetragonal ZrO_2 and θ-Al_2O_3. Similar results are observed after annealing $H_{25}AO$ at 1000 ^oC. A strong absorption band centered at ~490 cm^{-1} with a shoulder at 394 cm^{-1} is observed and is consistent with formation of tetragonal HfO_2. After annealing $H_{25}AO$ at 1100 and 1200 ^oC, distinctive vibrational modes on the broad absorption band attributable to θ-alumina and monoclinic HfO_2 are observed. The $H_{25}AO$ films annealed at 1100 and 1200 ^oC appear to be a mixture of θ-alumina, and monoclinic HfO_2. The $H_{25}AO$ films differ from the Z17AO films in that monoclinic HfO_2 forms more readily at lower temperatures than monoclinic ZrO_2.

In the FTIR spectrum of $Z_{50}AO$ films annealed at 350-500 ^oC (Fig. 5), and $H_{54}AO$ annealed at 350-800 ^oC (Fig. 7) annealed at 350-500 ^oC, a strong broad absorption band centered at 420 -440 cm^{-1} is observed and attributed to a mixture of γ-alumina and amorphous ZrO_2 or HfO_2. As the anneal temperature is increased, additional phase partitioning is observed. After annealing $Z_{50}AO$ at 800, 900, 1000, and 1100 ^oC, a strong absorption band centered at 440 cm^{-1} with a shoulder at 362 cm^{-1} and a weak absorption band at 140 cm^{-1} is observed and is consistent with formation of tetragonal ZrO_2. After annealing $Z_{50}AO$ at 1200 ^oC, distinctive vibrational modes are observed at 725, 572, 489, 447, 416, 347, 263, and 226 cm^{-1} and are attributed to monoclinic ZrO_2. After

annealing $H_{54}AO$ at 900 °C, a broad strong absorption band centered at 480 cm^{-1} is observed and is attributed to a mixture of γ-Al_2O_3 and tetragonal HfO_2. After annealing $H_{54}AO$ at 1000 °C, the absorption band at 480 cm^{-1} is broader with additional distinctive vibrational modes, suggestive of a mixture of θ-Al_2O_3 and monoclinic HfO_2. After annealing $H_{54}AO$ at 1200 °C, distinctive vibrational modes are observed at 735, 632, 601, 513, 411, 325, 255, 235, and 183 cm^{-1} and are attributed to monoclinic HfO_2. Again, monoclinic HfO_2 is observed to form more readily than monoclinic ZrO_2.

As shown in the FTIR spectrum of $H_{90}AO$ (Fig. 4), in the films annealed at 350-500 °C, a strong absorption band centered at 420 cm^{-1} is observed and attributed to and amorphous HfO_2. After annealing at 700, 800, and 900 °C, a strong absorption band centered at ~424 cm^{-1} with a shoulder at 355 cm^{-1} and a weak band at 250 cm^{-1} is observed and is consistent with formation of monoclinic HfO_2. After annealing at 900, 1000, and 1200 °C, distinctive vibrational modes attributable to monoclinic HfO_2 are observed. The $H_{90}AO$ films differ from pure HfO_2, in that tetraganol HfO_2 was observed after annealing at 700 and 800 °C, and the crystallization temperature of monoclinic HfO_2 was increased to 900 °C instead of 500 °C for pure HfO_2.

The average measured dielectric constant was 15 and 13 for the $Z_{17}AO$, and $Z_{50}AO$ films, respectively and 14 and 13 for the $H_{25}AO$ and $H_{54}AO$ films. A dielectric constant of 7 was observed for the $H_{90}AO$ films which was attributed to extensive oxidation of the underlying Si substrate increasing the interfacial oxide thickness and thus decreasing the dielectric constant. This hypothesis is consistent with the observation of very intense FTIR peaks attributed to SiO_2 in the $H_{90}AO$ films after annealing at 1000 °C for 30 minutes.

Discussion

In the XRD and FTIR spectrum of pure Al_2O_3 deposited by CSD, no crystallization of Al_2O_3 was observed until transformation into the α-Al_2O_3 phase after annealing at 1200 °C for 60

minutes. The lack of observed crystallization might be attributable to the persistent OH and H_2O content as observed in the FTIR spectrum of the Al_2O_3 films. Even after annealing the films at 1100 ^oC for 30 minutes, OH was still observed in the FTIR spectrum. Apparently crystallization and ordering of alumina is proceeded first by dehydroxylation and then by crystallization. In agreement with previous results,[19,20,26-29] we observed γ-Al_2O_3 at anneal temperatures $\leq$800 ^oC with variable amounts of OH and H_2O. θ-Al_2O_3 was observed at anneal temperatures of 900-1100 ^oC with reduced amounts of OH. Complete loss of OH was only observed after conversion into α-Al_2O_3 after annealing at 1200 ^oC.

As discussed in the literatue [19,20,26-29] the γ–θ phase transformations are continuous processes and it is very difficult to have pure phases. The γ–θ transitions are displacive or topotactive (the crystal structure transforms without destruction of the original crystal morphophogy) with the oxygen anion array remaining cubic close packed. The only structural changes being a redistribution of Al atoms between octahedral and tetrahedral sites.[33] The FTIR spectrum are consistent with this conjecture. Upon conversion to θ-Al_2O_3, an increased intensity of the absorption band at 540 cm^{-1} which is generally associated with octahedral vibrations is observed.

The final explusion of OH from the alumina matrix was only observed after transformation into α-Al_2O_3 after annealing at 1200 ^oC. The θ–α transition involves a reorganization of the oxygen atoms from a cubic close packing in the γ and θ phases to a denser hexagonal arrangement of oxygens. The transformation is associated with complete loss of tetrahedral sites and condensation of octahedral sites, thus accounting for the final expulsion of OH from the alumina matrix and the development of strong relatively narrow distinctive vibrational modes observed in the FTIR spectra of α-alumina indicative of an ordered microstructure.

At low ($\leq$25%) ZrO_2 or HfO_2 concentrations at anneal temperatures less than 900 ^oC, an amorphous γ-alumina like material was observed in the ZAO and HAO films, suggestive of a

nonequilbrium metastable mixture of Zr or Hf and Al. At higher ZrO_2 or HfO_2 concentrations or at higher anneal temperatures, phase partitioning of the ZAO and HAO films was observed in agreement with previously published results.[7-13,15-18] Tetragonal ZrO_2 or HfO_2 was observed to precipitate during transformation of γ-Al_2O_3 to θ-Al_2O_3, suggesting that Zr atoms are intimately bound within the γ-Al_2O_3 matrix.

In the $H_{90}AO$ films with 10% Al no evidence of alumina phase separation was observed by XRD or FTIR even after annealing at 1200 ^oC for 60 minutes suggesting a solubility of at least 10% Al in HfO_2. A dramatic alteration of transformation temperatures and stabilization of tetraganol HfO_2 was observed relative to pure HfO_2. In the $H_{90}AO$ films crystallization of tetragonal HfO_2 was observed after annealing at 700 and 800 ^oC. In contrast, pure HfO_2 was observed to only crystallize in the monoclinic phase at annealing temperatures $\geq$ 500 ^oC.

The average measured dielectric constants are 15 and 13 for the $Z_{17}AO$, and $Z_{50}AO$ films, respectively, and 14, 13, and 7 for the $H_{25}AO$, $H_{54}AO$, and $H_{90}AO$ films, respectively. The measured dielectric constant of 7 for the $H_{90}AO$ films is attributed to extensive oxidation of the underlying Si substrate, despite $H_{90}AO$ film thickness ranging from 1500 to 3900 Å. As shown in Figure 9, oxidation of the underlying Si increases with increasing HfO_2 content. The calculated area under the Si-O peaks at 1260 and 1070 cm^{-1} for the $H_{90}AO$ film is nine times as large as the same Si-O peak area for the $H_{17}AO$ film. Ytrria stabilized zirconia is a known oxgen conductor at elevated temperatures. Doping of zirconia with ytrria creates oxygen vacancies which play an essential role in the conductivity mechanism. A maximum in oxygen conduction is observed at 8% Y in the ZrO_2.[35,36,37,38,39,40] 10-25% Y doped HfO_2 is also a known ionic conductor at elevated temperatures.[41] Similiar oxygen conduction is speculated to occur in the HAO films with the $H_{90}AO$ film with 10% Al conducting more oxygen than the $H_{25}AO$ and $H_{54}AO$ films. To utilize

ZAO and HAO films in transistors, annealing conditions and stoichiometry will have to be carefully selected to not only minimize phase partitioning but also to avoid interfacial oxidation.

CONCLUSIONS

Crystallization and ordering of pure alumina was observed to proceed first by dehydroxylation and then by crystallization. We observed γ-Al_2O_3 at anneal temperatures $\leq$800 ^oC with variable amounts of OH and H_2O. θ-Al_2O_3 was observed at anneal temperatures of 900-1100 ^oC with reduced amounts of OH. Complete loss of OH was only observed after conversion into α-Al_2O_3 after annealing at 1200 ^oC.

Crystallization/phase separation of ZrO_2 and HfO_2 in ZAO and HAO films was observed to be concentration and annealing temperature dependent. At low ($\leq$25%) ZrO_2 or HfO_2 concentrations at anneal temperatures less than 900 ^oC, an amorphous γ-alumina like material was observed in the ZAO and HAO films. Phase partitioning of the ZAO and HAO films was observed at higher ZrO_2 or HfO_2 concentrations and at higher anneal temperatures. Combination of ZrO_2 and HfO_2 with Al_2O_3 in the ZAO and HAO films stabilized the tetragonal phase of ZrO_2 or HfO_2, and hindered the tetragonal to monoclinic transformation of ZrO_2 and HfO_2. Transformation from the tetragonal to monoclinic phase was observed to occur more readily at lower annealing temperatures in HAO films than ZAO films.

The dielectric constant of the $Z_{17}AO$ and $Z_{50}AO$ films and the $H_{25}AO$ and $H_{54}AO$ films was greater than the dielectric constant of Al_2O_3 alone. However, extensive oxidation of the underlying Si substrate was observed in the $H_{90}AO$ films and attributed to enhanced oxygen conduction at elevated temperatures. Therefore, to successfully utilize ZAO and HAO films in transistors, annealing conditions and stoichiometry will have to be carefully selected to not only minimize phase partitioning but also to avoid interfacial oxidation.

ACKNOWLEDGEMENTS

The author would like to acknowledge Sufi Zafar, Steve Cohen and Dave Klaus for electrical measurements.

.

Table 1. Annealing temperatures at which tetragonal (tet) and monoclinic (mc) ZrO_2 and HfO_2 and θ and α alumina are observed in the XRD or FTIR spectra of Al_2O_3, HfO_2, ZrO_2, ZAO and HAO films. n/o: not observed.

$Zr_xAl_{1-x}O_y$ x=	T °C	T °C	T °C	$Hf_xAl_{1-x}O_y$ x=	T °C	T °C	T °C
	tet ZrO_2	mc ZrO_2	Al_2O_3		tet HfO_2	mc HfO_2	Al_2O_3
Al_2O_3	-	-	1200(α)				
0.17	1,000	n/o	1000(θ)	0.25	1,000	1,100	1000(θ)
0.5	800	1,200	1200(θ)	0.54	900	1,000	1000(θ)
-	-	-	-	0.9	700	1,000	n/o
ZrO_2	500	900	-	HfO_2	n/o	500	-

FIGURE CAPTIONS

Figure 1. X-ray diffraction pattern of $H_{25}AO$ film annealed at 800, 900, 1000, 1100 and 1200 ^{o}C.

Figure 2. FTIR spectra of Al_2O_3 films after annealing at 350, 400, 500, 700, 800, 1000, 1100 ^{o}C for 30 minutes and 1200 ^{o}C for 60 minutes in flowing oxygen.

Figure 3. FTIR specta of $Z_{17}AO$, $Z_{50}AO$, $H_{25}AO$, $H_{54}AO$, and $H_{90}AO$ films after hot plate bake at 350 ^{o}C for 30 minutes in air.

Figure 4. FTIR spectra of $Z_{17}AO$ films after annealing at 350, 700, 800, 900, 1000, 1100 ^{o}C for 30 minutes and 1200 ^{o}C for 60 minutes in flowing oxygen.

Figure 5. FTIR spectra of $Z_{50}AO$ films after annealing at 350, 500, 800, 900, 1000, 1100 ^{o}C for 30 minutes and 1200 ^{o}C for 60 minutes in flowing oxygen.

Figure 6. FTIR spectra of $H_{25}AO$ films after annealing at 350, 700, 800, 900, 1000, 1100 ^{o}C for 30 minutes and 1200 ^{o}C for 60 minutes in flowing oxygen.

Figure 7. FTIR spectra of $H_{54}AO$ films after annealing at 350, 700, 800, 900, 1000 ^{o}C, and 1100 ^{o}C for 30 minutes in flowing oxygen.

Figure 8. FTIR spectra of $H_{90}AO$ films after annealing at 350, 500, 700, 800, 900, 1000 ^{o}C for 30 minutes and 1200 ^{o}C for 60 minutes in flowing oxygen.

Figure 9. FTIR spectra of $H_{25}AO$, $H_{54}AO$, and $H_{90}AO$ films after annealing at 1000 ^{o}C for 30 minutes in flowing oxygen with area under Si-O peak calculated.

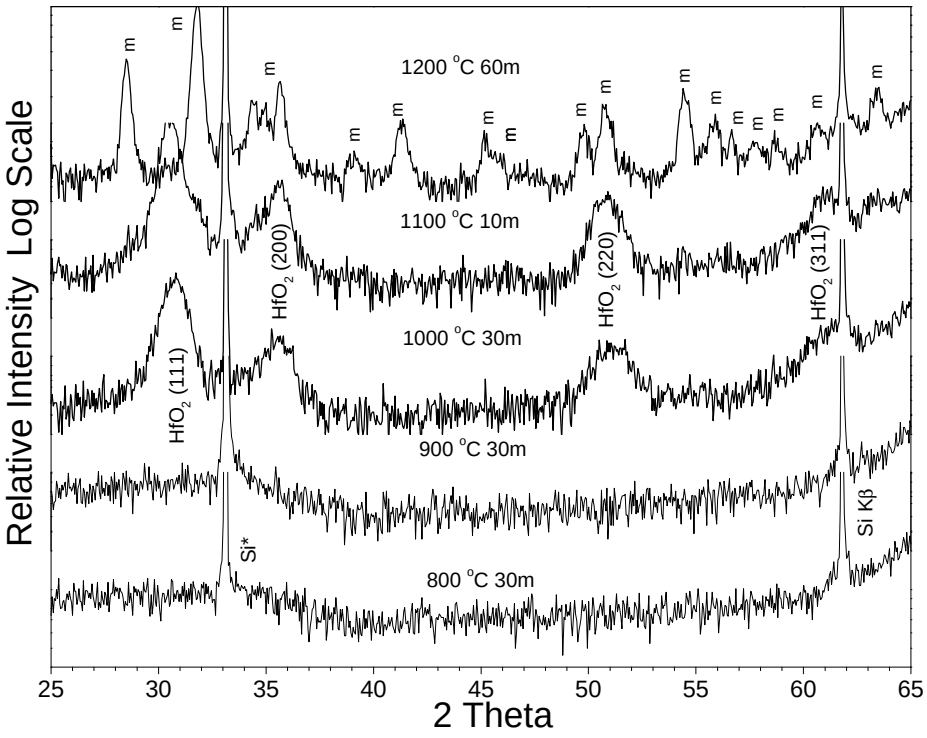

Figure 1. X-ray diffraction pattern of $H_{25}AO$ film annealed at 800, 900, 1000, 1100 and 1200 °C.

.

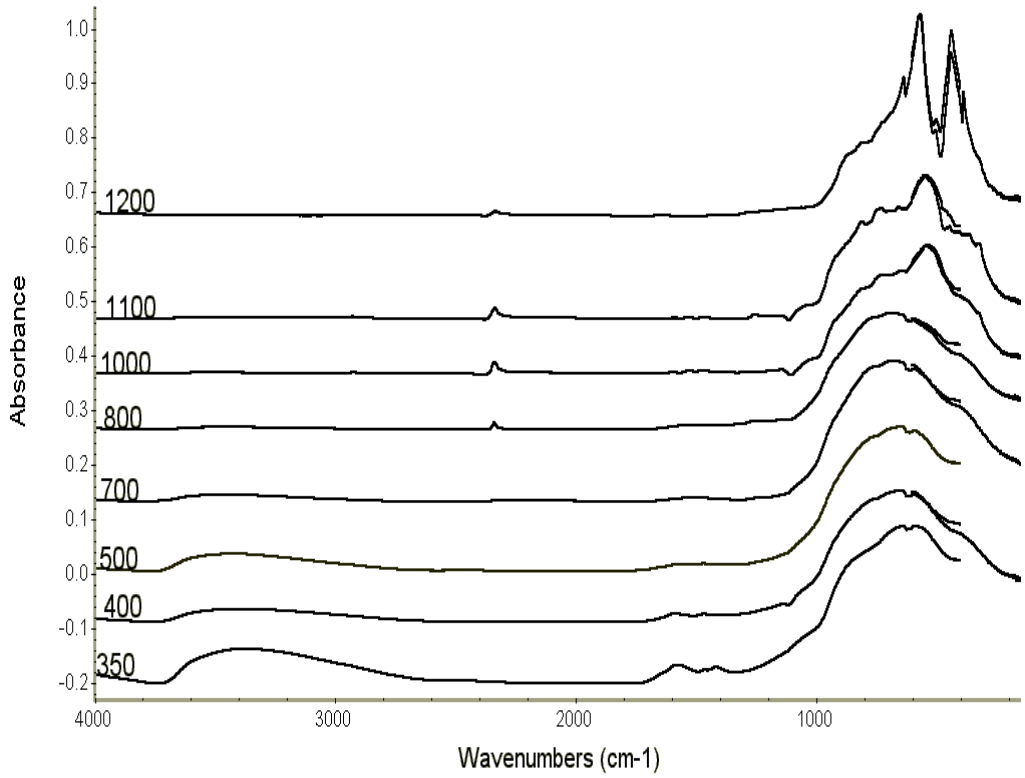

Figure 2. FTIR spectra of Al_2O_3 films after annealing at 350, 400, 500, 700, 800, 1000, 1100 ^oC for 30 minutes and 1200 ^oC for 60 minutes in flowing oxygen.

.

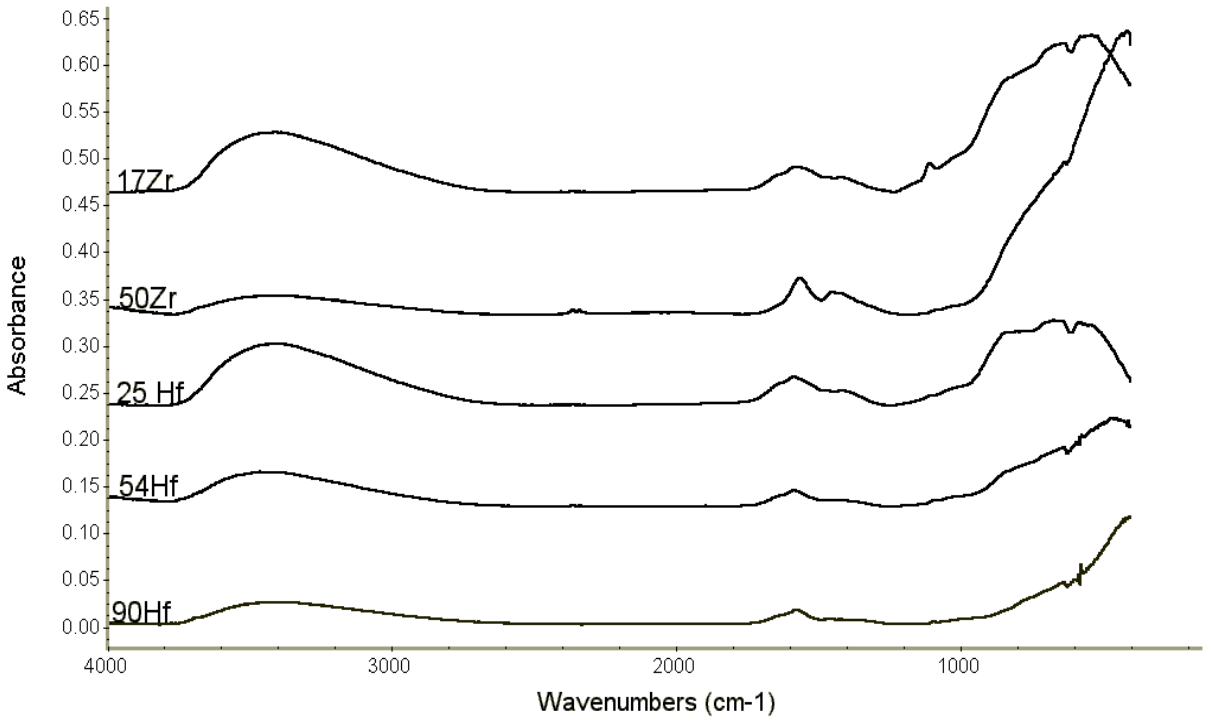

Figure 3. FTIR specta of $Z_{17}AO$, $Z_{50}AO$, $H_{25}AO$, $H_{54}AO$, and $H_{90}AO$ films after hot plate bake at 350 ºC for 30 minutes in air.

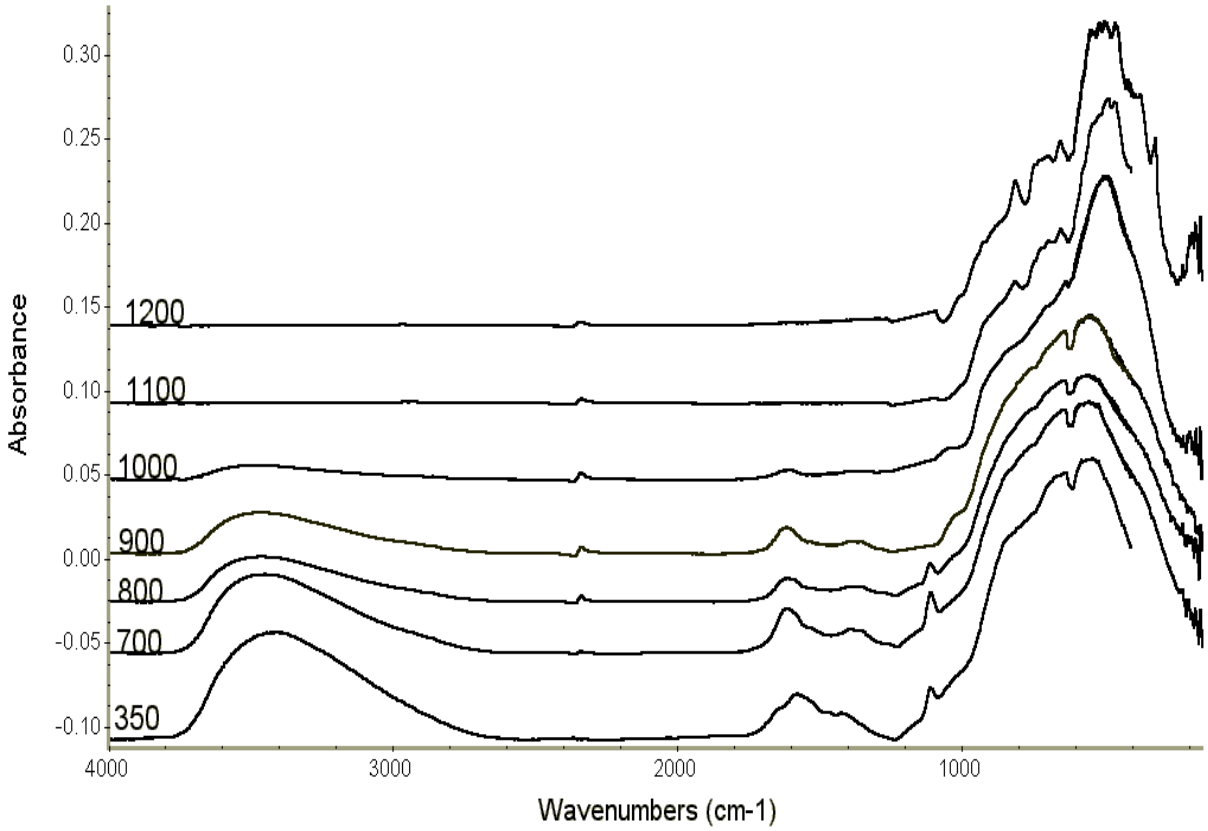

Figure 4. FTIR spectra of $Z_{17}AO$ films after annealing at 350, 700, 800, 900, 1000, 1100 ^{o}C for 30 minutes and 1200 ^{o}C for 60 minutes in flowing oxygen.

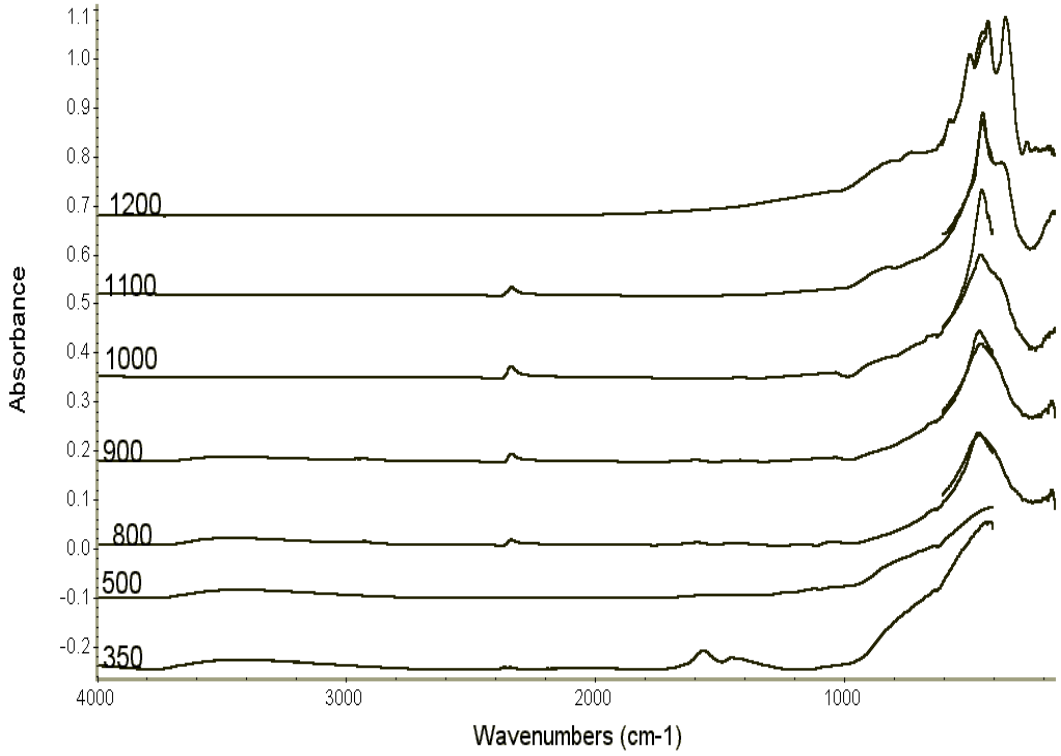

Figure 5. FTIR spectra of $Z_{50}AO$ films after annealing at 350, 500, 800, 900, 1000, 1100 ^{o}C for 30 minutes and 1200 ^{o}C for 60 minutes in flowing oxygen.

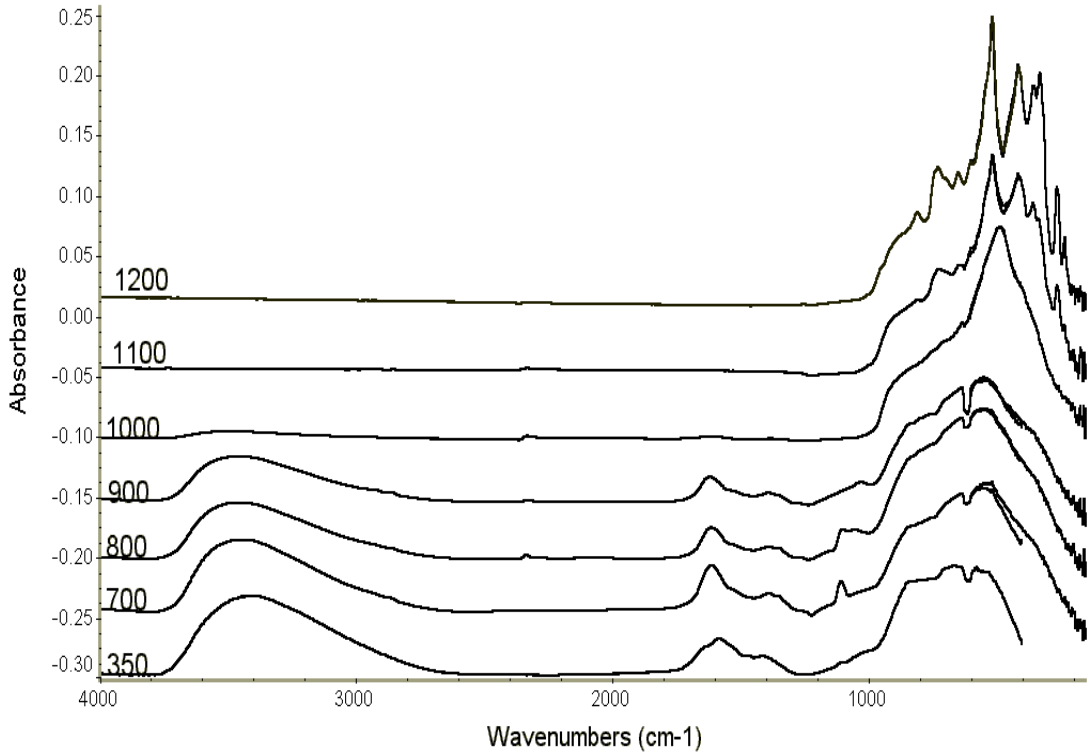

Figure 6. FTIR spectra of $H_{25}AO$ films after annealing at 350, 700, 800, 900, 1000, 1100 ^{o}C for 30 minutes and 1200 ^{o}C for 60 minutes in flowing oxygen.

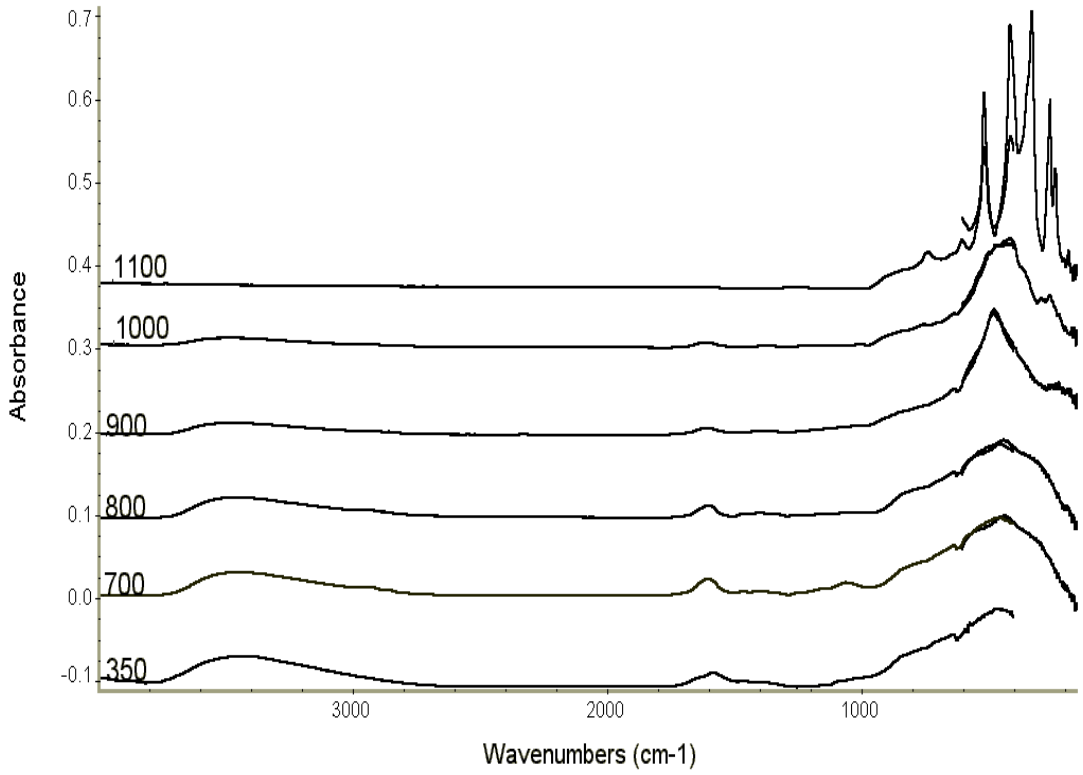

Figure 7. FTIR spectra of $H_{54}AO$ films after annealing at 350, 700, 800, 900, 1000 ^{o}C, and 1100 ^{o}C for 30 minutes in flowing oxygen.

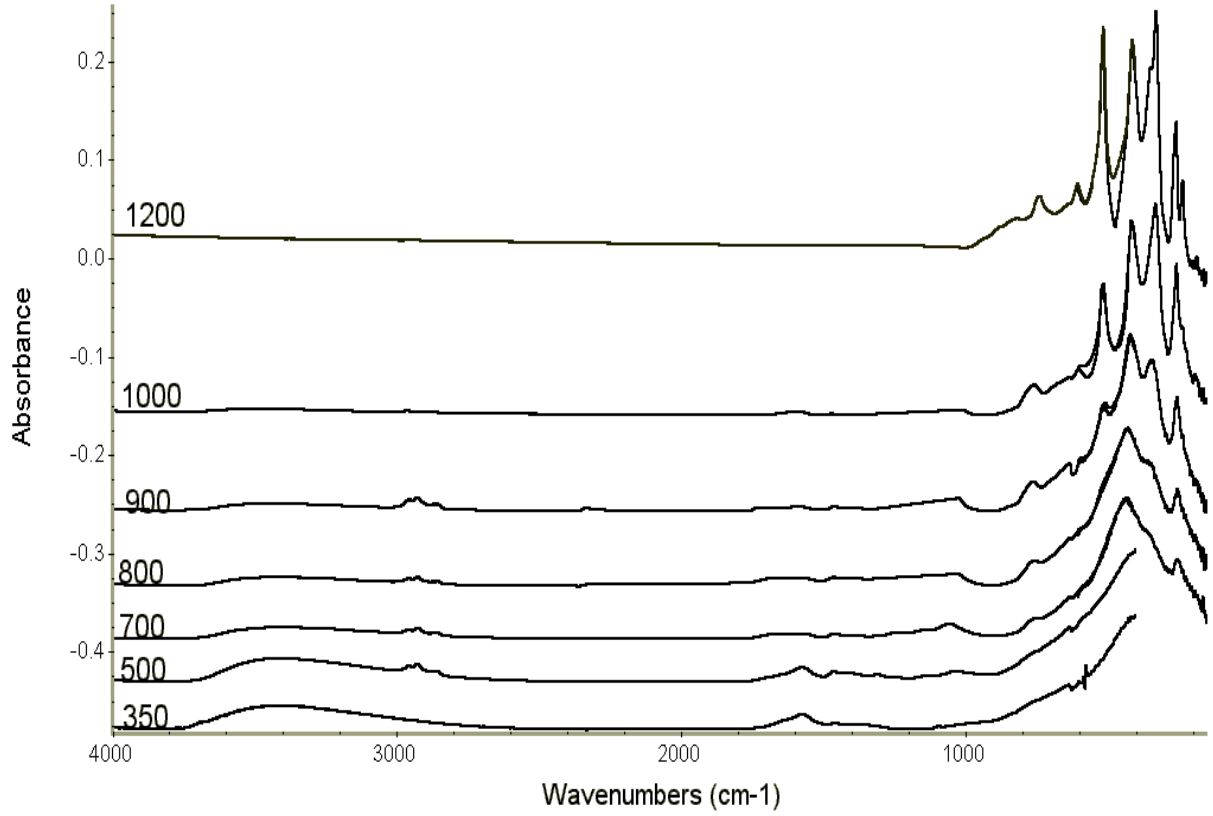

Figure 8. FTIR spectra of H_{90}AO films after annealing at 350, 500, 700, 800, 900, 1000 °C for 30 minutes and 1200 °C for 60 minutes in flowing oxygen.

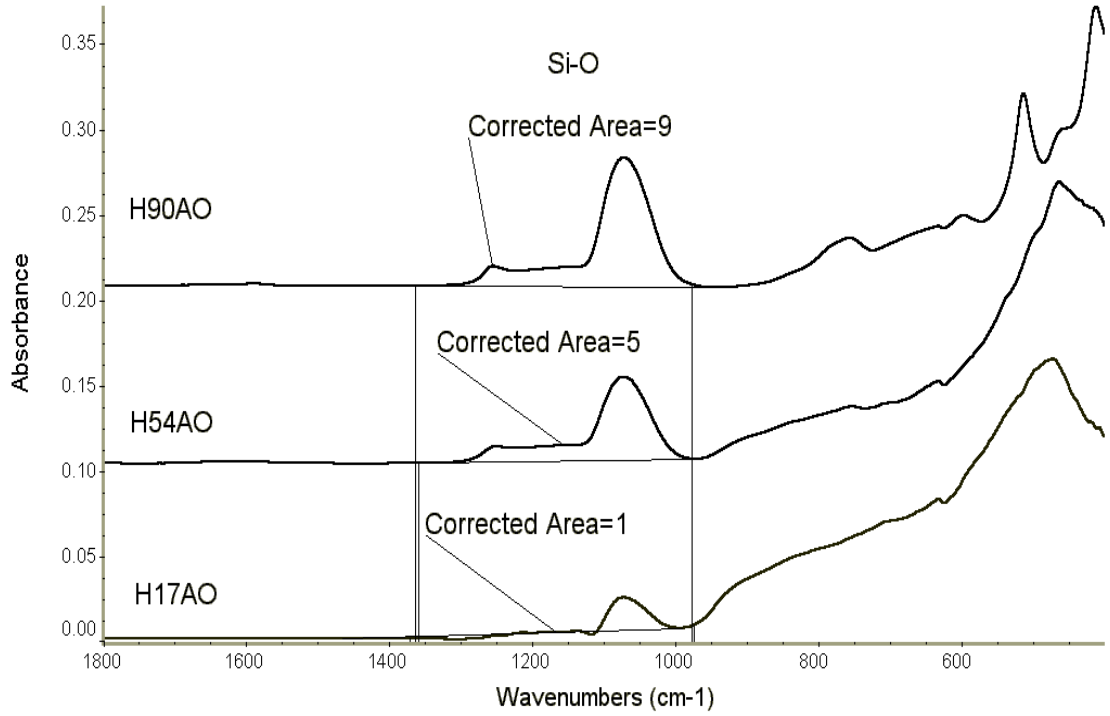

Figure 9. FTIR spectra of $H_{25}AO$, $H_{54}AO$, and $H_{90}AO$ films after annealing at 1000 ^{o}C for 30 minutes in flowing oxygen with area under Si-O peak calculated.

REFERENCES

1 G.D. Wilk, R.M. Wallace, J.M. Anthony, accepted to J. Appl. Physics

2 Billman, C.A. Tan, P.H. Hubbard, K.J. Schlom, D.G., Materials Research Society Symposium - Proceedings v 567 1999. p 409-414

3 L. Manchanda, W.H. Lee, J.E. Bower, F.H. Baumann, W.L. Brown, C.J. Case, R.C. Keller, Y.O. Kim, E.J. Laskowski, M.D. Morris, R.L. Opila, P.J. Silverman, T.W. Sorsch, G.R. Weber, IEDM, **21.6,** 1, (1998).

4 R.B. Van Dover, D.V. Lang, M.L. Green, L. Manchanda, in press J. Vac. Sci. Technol. (2001).

5 D.A. Neumayer, P.R. Duncombe, U.S. Patent No. 5 962 654 (5 October 1999).

6 D.A. Neumayer, P.R. Duncombe, U.S. Patent No. 6,002,031, (14 December 1999).

7 C. Li, Y.-W. Chen, T.-M. Yen, J. Sol-Gel Science and Technology, **4**, 205-212, (1995)

8 S. Moreau, M. Gervais, A. Douy, Solid State Ionics **101-103**, 625 (1997).

9 J. Klein and W. Maier, Chem. Mater. **11**, 2584 (1999).

10 L. Gao, Q. Liu, J.S. Hong, H. Miyamoto, S.D. DeLaTorre, A. Kakitsuji, K. Liddel, D.P. Thompson, J. Mater. Sci. **33**, 1399, (1998).

11 M.L. Balmer, F.F. Lange, V. Jayaram, C.G. Levi, J. Am. Ceram. Soc. **78**, 1489 (1995).

12 M.L. Balmer, F.F. Lange, C.G. Levi, J. Am. Ceram. Soc. **77**, 2069 (1994).

13 E.A. Pugar, P.E.D. Morgan, J. Am. Ceram. Soc. **69**, C120 (1986).

14 A. Callegari, E. Cartier, M. Gribelyuk, H. F. Okorn-Schmidt, T. Zabel, submitted to J. Appl. Phys.

15 D.A.Neumayer and E. Cartier, J. Appl. Phys. **90**, (2001)

16 Y. Murase, E. Kato, K. Daimon, J. Am. Ceram. Soc. **69**, 83 (1986).

17 M. Kagawa, M. Kikuchi, Y. Syono, J. Am. Ceram. Soc. **66**, 751 (1983).

18 F.F. Lange, M.M. Hirlinger, J. Am. Ceram. Soc. **67**, 164 (1984).

19 A.H. Heuer, N. Claussen, W.M. Kriven, M. Ruhle J. Am. Ceram. Soc. **65**, 642 (1982).

20 Ph. Colomban, J. Mater. Sci. **24**, 3002 (1989).

21 V.J. Ingram-Jones, R.C.T. Slade, T.W. Davies, J.C. Southern, S. Salvador, J. Mater. Chem. 6, 73

22 D.A. Neumayer, P.R. Duncombe, R.B. Laibowitz, A. Grill Integrated Ferroelectrics, **18**, 297 (1997).

23 H.S. Gopalakrishnamurthy, R. Subba Rao, T.R. Narayanan Kutty, J. Inorg. Nucl. Chem., **37**, 891 (1975).

24 V. Jayaraman, T. Gnanasekaran, G. Periaswami, Mater. Letters **30**, 157 (1997).

25 N. Ozer, J.P. Cronin, Y.-J. Yao, A.P. Tomsia, Solar Energy Mater. & Solar Cells, **59**, 355 (1999).

26 P. Tarte, Spectrochimica Acta, **23A**, 2127 (1967).

27 M.I. Baratron, P.J. Quintard, J. Mol. Struct. **79**, 337 (1982).

28 C.H. Shek, J.K.L. Lai, T.S. Gu, G.M. Lin Nanostructured Mater., **8**, 605 (1997).

29 G. Urretavizcaya, A.L. Cavalieri, J.M. Porto Lopez, I. Sobrados, J. Sanz, J. Mater. Synth. Process. **6[1]**, 1 (1998).

30 J.M. Saniger, Mater. Lett., **22**, 109 (1995).

31 G. Busca, V. Lorenzelli, G. Ramis, R.J. Willey, Langmuir **9**, 1492 (1993).

32 P. Raharjo, C. Ishizake, K. Ishizaki, J. Ceram. Soc. Jap. **108**, 1 (2000).

33 M.C. Stegmann, D. Viven, C. Mazieres, Spectochimica Acta, **29A**, 1653 (1973).

34 K. Sinko, R. Mezei, J. Rohonczy, P. Fratzl, Langmuir, **15**, 6631 (1999).

35 T.H. Etsell and S.N. Flengas, Chem Rev. **70**, 339 (1970).

36 E.C. Subbarao, H.S. Maiti, Solid State Ionics, **11**, 317 (1984).

37 C.R.A Catlow J. Chem. Soc. Faraday Trans. **86** 1167 (1990).

38 J.P. Goff, W. Hayes, S. Hull, M.T. Hutchings, K.N. Clausen Phys Rev. B **59,** 14202 (1999)

39 Y. Yamamura, S. Kawasaki, H. Sakai, Solid State Ionics, **126,** 181 (1999)

40 M. S. Khan, M. S. Islam, D.R. Bates, J. Mater. Chem. **8**, 2299 (1998).

41 J.E. Zhuiykov, Ceram. Soc. **20,** 967 (2000).